

## Subband mixing rules in circumferentially perturbed carbon nanotubes: Effects of transverse electric fields

Yong-Hyun Kim and K. J. Chang

*Department of Physics, Korea Advanced Institute of Science and Technology, Taejon 305-701, Korea*

(Received 5 July 2001; published 14 September 2001)

We analyze various potential environments such as electrodes, substrates, gate voltages, and flattening deformations in single-wall C nanotubes in terms of circumferential perturbations on nanotube surfaces. Considering the periodicity of perturbations, we derive selection rules in the subband mixing caused by perturbations. Uniform electric fields perpendicular to the tube axis induce band-gap modification such as opening and closure. Thus, locally applied transverse fields cause significant backscattering of the states near the threshold for transmission.

DOI: 10.1103/PhysRevB.64.153404

PACS number(s): 73.22.-f, 73.63.Fg, 85.35.Kt, 71.20.Tx

In transport measurements, single-wall carbon nanotubes are usually placed in various potential environments such as metal electrodes, liquid metal baths, oxide substrate, gate potentials, and flattening deformations.<sup>1</sup> These environments give rise to extra potentials on the C atoms on the nanotube surface, and thus influence the electronic and transport properties of nanotubes. Multiwall nanotubes deposited over metal electrodes exhibit diffusive transports,<sup>2</sup> while a ballistic transport appears to be the dominant conduction for those in liquid metal baths.<sup>3</sup> Despite several theoretical attempts,<sup>4</sup> the puzzling observations of the two different conduction mechanisms are not resolved yet. Moreover, to our knowledge, the effect of gate voltages on the transport behavior has never been studied, although understanding this effect is important for device applications. Very recent calculations showed that flattening deformations induce the band-gap modification such as opening and closure,<sup>5,6</sup> and demonstrated that locally deformed nanotubes behave as quantum dots or wires.<sup>7</sup>

In this paper we investigate the effect of various environments such as flattening deformations, transverse electric fields, and electrodes on the electronic and transport properties of single-wall carbon nanotubes through first-principles pseudopotential and tight-binding calculations. Using a perturbative approach, we analyze the periodicity of external potentials along the circumferential direction, and find that selection rules exist in subband mixings. For the (17,0) and (40,0) tubes under electric fields perpendicular to the tube axis, both the tubes undergo a semiconductor-metal transition, while the band gap of the (40,0) nanotube with a larger diameter decreases more rapidly. On the other hand, in the metallic (18,0) tube, a gap is generated near the Fermi level, resulting in zero transmission. We investigate the effects of transverse electric fields on total transmission and find that locally applied fields cause significant backscattering of the incident channels going from field-free to field-exposed regions, especially for large diameter tubes.

A single-wall nanotube (SWNT) is constructed by wrapping up a graphite sheet into a cylinder. Because of the periodicity along the circumference  $L$ , the wave vector  $k_x$  along the circumferential direction  $x$  on the graphite sheet is quantized by the rule  $k_x = 2\pi n/L$ , where  $n$  is an integer. Then, each subband is represented by  $|n\rangle$  with the Bloch phase

$\exp(i2\pi nx/L)$ . Combined with the quantization rule for  $k_x$ , the electronic structure of nanotubes with very large diameters, where the curvature effects are negligible, are easily understood from the Hamiltonian for a graphite sheet.<sup>8</sup> If tube diameters are small, the curvature effect can be included by considering a perturbing potential on the nanotube surface. Similarly, for other environments such as metal electrodes, gate fields, and flattening deformations, we can also consider their perturbing potentials along the circumference. If a perturbing potential  $\mathbf{V}(x)$  has a period of  $L$ , it can be expanded in a Fourier series,

$$\mathbf{V}(x) = \sum_{k_x \in \text{FBZ}} e^{ik_x x} \left[ \sum_G \mathbf{V}(k_x + G) e^{iGx} \right], \quad (1)$$

where  $G$ 's are the reciprocal lattice vectors and  $k_x$ 's are restricted to the first Brillouin zone (FBZ). Then, the mixing of an unperturbed state  $|n\rangle$  to the first order is expressed as

$$|n\rangle \rightarrow |n\rangle + \sum_{n' \neq n} |n'\rangle \frac{\langle n | \mathbf{V} | n' \rangle}{\epsilon_n - \epsilon_{n'}}, \quad (2)$$

where  $\epsilon_n$  denotes the eigenvalue of  $|n\rangle$ . If the perturbing potential has a Fourier component of  $k_x = 2\pi m/L$  in Eq. (1), the matrix elements in Eq. (2) are nonvanishing for  $\Delta n (= n - n') = m$ , from which selection rules are determined in the subband mixing for various perturbing potentials.

If the inherent surface curvature of a nanotube is considered as a perturbing potential, the subband mixing is only allowed between two states with  $\Delta n = 0$ , because of the rotational symmetries about the tube axis. In nanotubes, these two states correspond to  $|n_\sigma\rangle$  and  $|n_\pi\rangle$ , which have the same  $n$  but different energies. From the subband mixing rule, we can easily understand the so-called rehybridization between the  $\sigma$  and  $\pi$  states due to the curvature effect.<sup>9</sup> In SWNT's with very small diameters, it is well known that the  $\sigma^* - \pi^*$  hybridization occurs between two singlet states, which are denoted by  $|0_{\sigma^*}\rangle$  and  $|0_{\pi^*}\rangle$ , giving rise to metallic conduction.<sup>10</sup>

For flattening deformations,<sup>5</sup> its perturbing potential has the period of  $L/2$  along the circumferential direction [see Fig. 1(a)]. Thus, the subband mixing occurs between states with

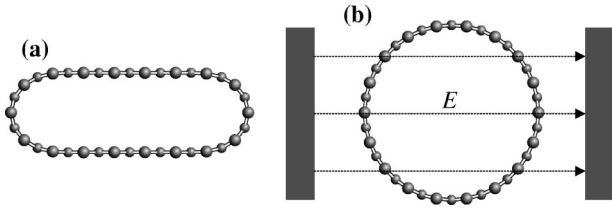


FIG. 1. (a) A cross-sectional view of a flattened zigzag tube. (b) Uniform electric fields  $E$  are applied for a zigzag tube placed between two parallel metal plates.

$\Delta n = 0$  and  $\pm 2$ . For  $\Delta n = 0$ , the subband mixing is similar to that caused by the curvature effect, while for  $\Delta n = \pm 2$ , additional  $\pi$ - $\pi$  hybridizations occur between two  $\pi$  states such as  $|0_{\pi}\rangle$  and  $|\pm 2_{\pi}\rangle$ . This simple rule is consistent with the results of previous first-principles calculations for flattened nanotubes,<sup>5</sup> which showed that flattening deformation eventually closes the band gap of zigzag nanotubes. This gap closure is attributed to the fact that the singlet state  $|0_{\pi^*}\rangle$  strongly mixed with the  $|\pm 2_{\pi^*}\rangle$  states decreases under flattening deformation, with the electron charge densities localized in the curved regions. In flattened nanotubes, the  $n = \pm 1$  states are also hybridized by flattening deformation,<sup>6</sup> resulting in the mixed state of  $|1_{\pi^*}\rangle$  and  $|-1_{\pi^*}\rangle$ , while these states are degenerate in perfect tubes. We point out that in the mixing of  $|0_{\pi}\rangle$  and  $|\pm 2_{\pi}\rangle$ , the energy difference in Eq. (2) is much smaller, as compared to the  $\sigma$ - $\pi$  hybridization induced by the selection rule of  $\Delta n = 0$ . Thus, the band-gap modification by flattening deformation is appreciable even in the metallic (18,0) nanotube, while the inherent curvature effect is negligible for zigzag ( $N,0$ ) nanotubes with large diameters ( $N > 9$ ).

When nanotubes are placed on a  $\text{SiO}_2$  substrate, they experience perturbing potentials by gate voltages applied to the substrate. Then, we can simply assume that the perturbing potential is represented by uniform transverse electric fields, as shown in Fig. 1(b). Considering the period  $L$  of the perturbing potential along the circumference, we find that the matrix elements in Eq. (2) are nonzero for  $\Delta n = 0$  and  $\pm 1$ . To see the effect of transverse electric fields on the band structure, we perform first-principles pseudopotential calculations. Here norm-conserving pseudopotentials are generated by the scheme of Troullier and Martins,<sup>11</sup> and the Ceperley-Alder exchange and correlation potential<sup>12</sup> is used within the local-density-functional approximation (LDA). We also perform tight-binding (TB) calculations with the Slater-Koster-type nonorthogonal basis.<sup>13</sup> For a uniform electric field  $E$  along the  $y$  axis perpendicular to the tube axis, we add a perturbing potential  $V = -eEy$  to the onsite energies of carbon atoms in TB calculations, while in LDA calculations we use a sawtooth-type local potential for a supercell geometry. Figure 2 shows the calculated TB band structures (for simplicity,  $|\pm n\rangle$  states are denoted by  $|n\rangle$ ) of the (17,0) zigzag tube under uniform electric fields. Because of the denominator in Eq. (2), crossed or almost degenerate bands are strongly affected by electric fields. In fact, we find that the crossed  $|6\rangle$  and  $|7\rangle$  states are split under a very small field of  $E = 0.03 \text{ V/\AA}$  in both the valence and conduction bands, and the almost degenerated  $|0\rangle$ ,  $|1\rangle$ , and  $|2\rangle$  states are

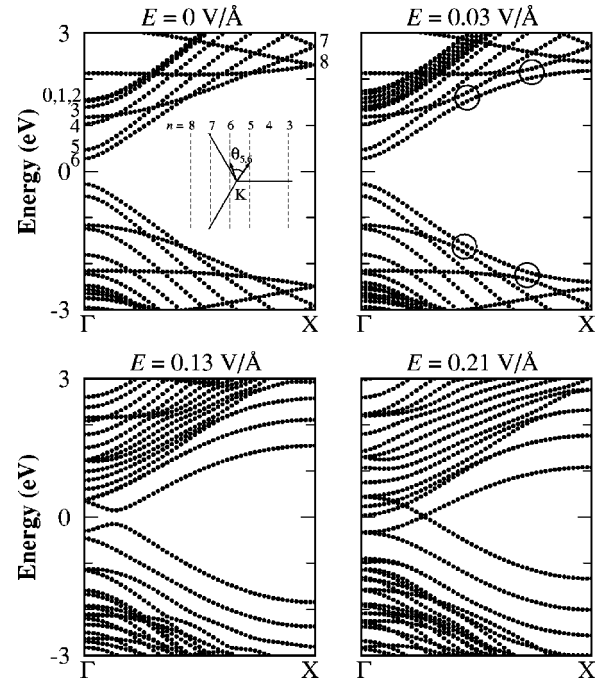


FIG. 2. Tight-binding band structures of the (17,0) SWNT under various transverse electric fields. The inset shows the zone boundaries (solid lines) near the symmetric  $K$  point in the two-dimensional Brillouin zone of the graphite sheet, the allowed  $\mathbf{k}$ -point lines ( $n = 3-8$ ), and the angle  $\theta_{5,6}$  between two wave vectors indicating the Bloch states  $|5\rangle$  and  $|6\rangle$ . The subbands are numbered by  $n$  on the allowed  $\mathbf{k}$ -point lines. Open circles in the upper-right panel indicate the energy splittings of the crossed bands due to electric fields.

broadened. A similar splitting is also found for the crossed  $|7\rangle$  and  $|8\rangle$  states. As the field strength increases, the energy splitting and broadening become more significant.

In addition, we find that the band-edge states, which correspond to  $|6_v\rangle$  and  $|6_c\rangle$  in the valence and conduction bands, respectively, move away from the  $\Gamma$  point, as shown in Fig. 2. These band-edge states are found to be eventually crossed with each other, resulting in a semiconductor-metal transition. The movement of the band edge states can be understood by the relation  $\langle n | \mathbf{V} | n' \rangle \sim V(n-n') \cos(\theta_{n,n'}/2)$  in the  $\mathbf{k} \cdot \mathbf{p}$  approximation,<sup>14,15</sup> where  $\theta_{n,n'}$  is the angle between two wave vectors to be mixed, as indicated in Fig. 2. In the (17,0) tube, since  $\theta_{5,6}$  is  $180^\circ$  at the  $\Gamma$  point, the mixing between  $|5\rangle$  and  $|6\rangle$  is prohibited. Thus, the  $|6_v\rangle$  and  $|6_c\rangle$  states are almost unaffected by electric fields at the  $\Gamma$  point. However, away from the  $\Gamma$  point, since  $\theta_{5,6}$  is less than  $180^\circ$ , the  $|6_v\rangle$  and  $|6_c\rangle$  states can be mixed with the  $|5\rangle$  state, moving into and eventually closing the original band gap. We find that the hybridized singlet state, i.e., a mixed state of  $|0\rangle$  and  $|1\rangle$ , decreases with increasing of the field strength, and moves into the original gap region at  $E = 0.21 \text{ V/\AA}$ . This behavior is very similar to the energy lowering of the hybridized singlet state found in zigzag SWNT's with small diameters<sup>10</sup> and in flattened zigzag tubes,<sup>5</sup> which closes the original band gap. Testing various zigzag tubes, we note that the hybridized singlet state moves into the original band gap for  $N < 17$ , inducing the

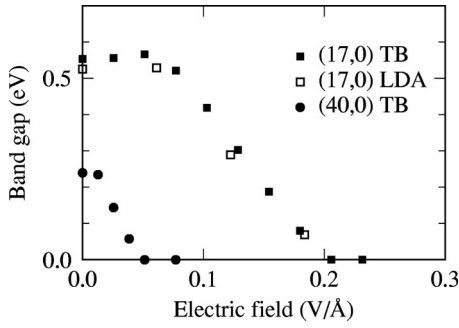


FIG. 3. The LDA and TB band gaps are plotted as a function of field strength for the (17,0) and (40,0) tubes.

semiconductor-metal transition before the band gap is affected by the movement of the band edges. For the (17,0) and (40,0) semiconducting SWNT's with diameters of 1.4 and 3.2 nm, respectively, the band gaps are plotted as a function of field strength in Fig. 3. LDA and TB calculations give quite similar results. As the field strength increases, both the (17,0) and (40,0) tubes exhibit the semiconductor-metal transition. Since the energy differences between neighboring subbands are smaller for nanotubes with larger diameters, the electronic structure of the (40,0) tube is more sensitive to external perturbations. For the (40,0) tube, the semiconductor-metal transition occurs at a lower electric field of  $E=0.05$  V/Å whereas  $E=0.21$  V/Å for the (17,0) tube.

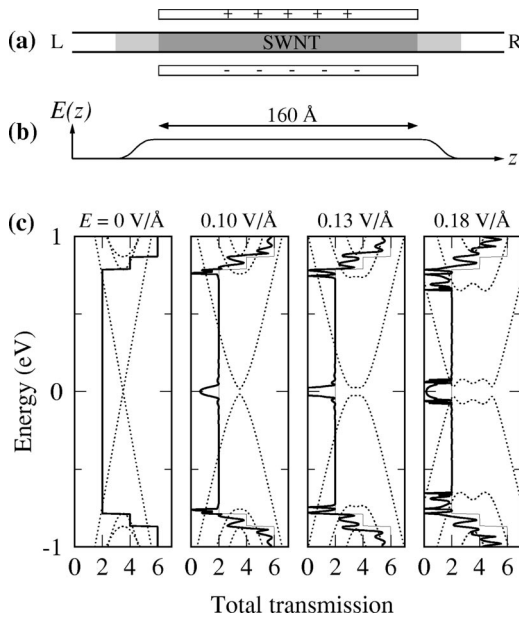


FIG. 4. (a) A schematic view of a nanotube device, where transverse electric fields are applied locally for the (18,0) nanotube between two parallel metal plates. Here L and R denote the left and right leads, respectively. (b) The electric fields are uniform inside the metal plates with the length of 160 Å, while they decay gradually to zero outside the plates. (c) Total transmissions (solid lines) through the nanotube device as a function of energy, with the Fermi level referenced to zero. Dotted lines denote the band structures of the (18,0) tube near the Fermi level for various field strengths.

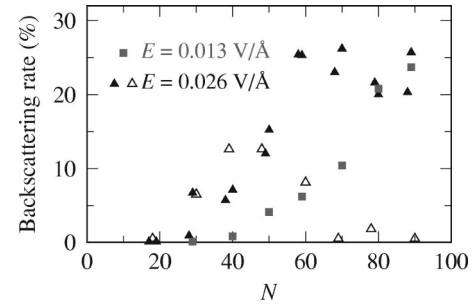


FIG. 5. Backscattering rates are drawn for various  $(N,0)$  nanotubes. Filled squares and triangles denote semiconducting tubes, while empty triangles denote metallic tubes.

Next, we examine the transport properties of metallic nanotubes under local transverse electric fields. We consider the (18,0) SWNT placed between two parallel metal plates [see Fig. 4(a)], where the curvature effect is much smaller than the perturbation due to electric fields. For energies near the Fermi level, since subband mixings occur between neighboring  $\pi$  states, we employ the  $\pi$ -orbital approximation. Assuming that electric fields are uniform between the metal plates with the length of 160 Å but decay gradually to zero outside the plates, as shown in Fig. 4(b), we calculate the total transmission through the nanotube with use of the Green's function approach.<sup>16,17</sup> The calculated band structures and total transmissions are drawn in Fig. 4(c). We find that electric fields create a gap of 0.03 eV at  $E=0.1$  V/Å, which gives rise to a transmission barrier. As the field strength increases, this gap is enlarged up to 0.06 eV, resulting in zero transmission. Based on our results, we propose that this nanotube device may act as a quantum switch for transverse electric fields of  $E=0.1-0.2$  V/Å. Here we point out that for metallic zigzag tubes with larger diameters such as (39,0) and (60,0) tubes, small gaps are closed again by the movement of subbands in the gap region, as addressed for the (40,0) tube.

Finally, we discuss the effect of layout geometries on the subband mixing in conductance measurements of multiwall nanotubes. In usual back-gated geometries with side contacts,<sup>2</sup> where diffusive transports were reported, the matrix elements in Eq. (2) are nonzero for  $\Delta n = \pm 1$ , similar to the uniform field case. On the other hand, multiwall nanotubes in liquid metal contacts, which showed ballistic transports, satisfy the selection rule of  $\Delta n = 0$ , because of the rotational symmetries about the tube axis. In this case, the electronic structures of the outermost shells are expected to be robust to liquid metal contacts because the energy difference between the  $|n_\sigma\rangle$  and  $|n_\pi\rangle$  states is very large. Thus, liquid metal contacts may not affect the quantum coherent transport. In the case of side contacts, small energy differences between neighboring  $\pi$  bands lead to severe subband mixings that may give rise to scattering centers for electron conduction. For various  $(N,0)$  nanotubes, we examine the backscattering rate of incident channels at the boundary between field-free and field-exposed regions; the electric field is assumed to be supplied by side contacts as discussed before. To exclude possible short-range scatterings,<sup>15</sup> we include a buffer region of about 20 Å at the boundary, where

the electric field increases gradually from zero. For electric fields of  $E=0.013$  and  $0.026$  V/Å, the calculated backscattering rates are plotted in Fig. 5; the backscattering rate is estimated by averaging the total transmissions over the energy range of  $0.04$  eV from the valence band edge, where only two channels exist. In semiconducting tubes with  $N \leq 28$ , backscattering rates are found to be very low for  $E = 0.026$  V/Å, while they increase to  $\sim 25\%$  for nanotubes with larger diameters. For smaller electric fields of  $E = 0.013$  V/Å, we find appreciable backscattering rates in semiconducting tubes with  $N \geq 50$ . In metallic tubes, the backscattering rate depends on the existence of the band gap; as the diameter increases, i.e.,  $N \geq 69$ , the band gaps developed by electric fields are closed again, resulting in very low backscattering rates. On basis of our results, we suggest that in the outermost shells with diameters of  $10\text{--}20$  nm

( $N > 120$ ) electrons will be easily scattered by the fluctuation of electric fields.

In conclusion, we have studied in a perturbative way the effect of various potential environments on the electronic structure of SWNT's, and find selection rules in the subband mixing caused by perturbed potentials. When single-wall nanotubes are placed on a substrate, applied gate voltages affect the band structure by producing transverse electric fields; semiconducting tubes undergo a semiconductor-metal transition as the field strength increases, while band gaps are generated in metallic tubes. We suggest that the fluctuation of transverse electric fields due to a substrate causes significant backscattering of the states near the threshold for transmission.

This work is supported by the QSRC at Dongguk University.

<sup>1</sup>C. Dekker, Phys. Today **52** (5), 22 (1999).

<sup>2</sup>L. Langer *et al.*, Phys. Rev. Lett. **76**, 479 (1996); C. Schönberger Appl. Phys. A **69**, 283 (1999); A. Bachtold *et al.*, Nature (London) **397**, 673 (1999); A. Bachtold *et al.*, Phys. Rev. Lett. **84**, 6082 (2000).

<sup>3</sup>S. Frank, P. Poncharal, Z.L. Wang, and W.A. de Heer, Science **280**, 1744 (1998).

<sup>4</sup>H.J. Choi, J. Ihm, Y.-G. Yoon, and S.G. Louie, Phys. Rev. B **60**, R14 009 (1999); S. Sanvito, Y.-K. Kwon, D. Tománek, and C.J. Lambert, Phys. Rev. Lett. **84**, 1974 (2000).

<sup>5</sup>C.-J. Park, Y.-H. Kim, and K.J. Chang, Phys. Rev. B **60**, 10 656 (1999).

<sup>6</sup>Y.-H. Kim, C.-J. Park, and K.J. Chang, J. Korean Phys. Soc. **37**, 85 (2000).

<sup>7</sup>H.-S. Sim, C.-J. Park, and K.J. Chang, Phys. Rev. B **63**, 073402 (2001).

<sup>8</sup>M.S. Dresselhaus, G. Dresselhaus, and P.C. Eklund, *Science of*

*Fullerenes and Carbon Nanotubes* (Academic, San Diego, 1996).

<sup>9</sup>N. Hamada, S. Sawada, and A. Oshiyama, Phys. Rev. Lett. **68**, 1579 (1992).

<sup>10</sup>X. Blase, L.X. Benedict, E.L. Shirley, and S.G. Louie, Phys. Rev. Lett. **72**, 1878 (1994).

<sup>11</sup>N. Troullier and J.L. Martins, Phys. Rev. B **43**, 1993 (1991).

<sup>12</sup>D.M. Ceperley and B.J. Alder, Phys. Rev. Lett. **45**, 566 (1980).

<sup>13</sup>M.J. Mehl and D.A. Papaconstantopoulos, Phys. Rev. B **54**, 4519 (1996).

<sup>14</sup>T. Ando, T. Nakanishi, and R. Saito, J. Phys. Soc. Jpn. **67**, 2857 (1998).

<sup>15</sup>P.L. McEuen, M. Bockrath, D.H. Cobden, Y.-G. Yoon, and S.G. Louie, Phys. Rev. Lett. **83**, 5098 (1999).

<sup>16</sup>S. Datta, *Electronic Transport in Mesoscopic Systems* (Cambridge University Press, Cambridge, 1995).

<sup>17</sup>M.P. Anantram and T.R. Govindan, Phys. Rev. B **58**, 4882 (1998).